Three-Dimensional Shallow Water Acoustics

Dr. Ying-Tsong Lin
Applied Ocean Physics and Engineering Department
Woods Hole Oceanographic Institution
Woods Hole, MA 02543
phone: (508) 289-2329   fax: (508) 457-2194   email: ytlin@whoi.edu

LONG-TERM GOALS

Both physical oceanographic processes and marine geological features in the areas of continental shelf and shelfbreak can cause horizontal heterogeneity in medium properties, so horizontal refraction and reflection of sound can occur and produce significant three-dimensional (3-D) sound propagation effects. The long-term goals of this project are targeted on understanding the 3-D acoustic effects, and their temporal and spatial variability, caused by the environmental factors existing commonly in the continental shelf and shelfbreak areas, such as slopes, submarine canyons, sub-bottom layers, surface waves, internal waves and shelfbreak fronts.

OBJECTIVES

One of the research objectives in this project is to develop efficient and accurate numerical models for studying underwater sound propagation in complex ocean environments. The ultimate scientific objective is to study the underlying physics of the 3-D sound propagation effects caused jointly by physical oceanographic processes and geological features. To achieve this goal, individual environmental factor will be first studied and then considered jointly with a unified ocean, seabed and acoustic model. Another major objective is to develop a tangent linear model to predict acoustic fluctuations and derive sound pressure sensitivity kernels due to 3-D sound speed perturbation in the water column. The sensitivity analysis will consider both the joint ocean and seabed effects.

APPROACH

The technical approaches employed in the 3-D sound propagation study include **theoretical analyses**, **numerical computation**, **real data analyses** and **field work experiments**. A 3-D normal mode method has been used to study canonical environmental models of shelfbreak front systems [1] and nonlinear internal wave ducts [2-3]. 3-D parabolic-equation wave propagation models with improved split-step marching algorithms [4-6] are used to study sound propagation in realistic environments.

The parabolic-equation (PE) approximation method, first introduced by Tappert [1] to underwater sound propagation modeling, has long been recognized as one of the most efficient and effective numerical methods to predict sound propagation in complex environments. The advantage of this method is due to the fact that it converts the Helmholtz wave equation of elliptic type to a one-way wave equation of parabolic type. The conversion allows efficient marching solution algorithms for

solving the boundary value problem posed by the Helmholtz equation. This can reduce significantly the requirement for computational resources, especially for modeling three-dimensional (3-D) sound propagation.

A higher order numerical algorithm has been proposed to split the square-root Helmholtz operator employed by the PE method for modeling sound propagation. This operator splitting method deals with multidimensional cross terms to yield a more accurate approximation, and, most importantly, it still permits efficient 3-D PE numerical solvers, such as the Split-Step Fourier method [5] and the Alternative Direction Implicit (ADI) Padé method [6]. The higher order operator splitting algorithm is shown in the next equation:

$$\sqrt{k_{ref}^{-2}\nabla_{\perp}^2 + n^2} = \sqrt{1 + \varepsilon + \mu} = -1 + \sqrt{1+\varepsilon} + \sqrt{1+\mu} - \frac{1}{2}\left(-1 + \sqrt{1+\varepsilon}\right)\left(-1 + \sqrt{1+\mu}\right)$$
$$- \frac{1}{2}\left(-1 + \sqrt{1+\mu}\right)\left(-1 + \sqrt{1+\varepsilon}\right),$$
(1)

where $k_{ref} = \omega/c_{ref}$ is the reference wavenumber, n is the index of refraction $n = c_{ref}/c = k/k_{ref}$, and $\nabla_{\perp}^2$ denotes the Laplacian operating on the transverse coordinates.

Another numerical method to be utilized is a tangent linear solution to predict acoustic fluctuations due to 3-D sound speed perturbation in the water column. This model has been developed and published [8], and it is briefed here along with an application to determine the sensivitiy kernel of sound pressure variability due to changes in medium sound speed. Consider the one-way parabolic wave equation,

$$\frac{\partial}{\partial x}u(x,y,z) = ik_{ref}\left\{-1 + \sqrt{k_{ref}^{-2}\nabla_{\perp}^2 + n^2(x,y,z)}\right\}u(x,y,z),$$
(2)

where $u = p\exp(-ik_{ref}x)$, p is the sound pressure, k_{ref} is the reference wavenumber, and n is the index of refraction with respect to k_{ref}. Now, denote the exact PE operator as the following

$$\mathcal{L} = -1 + \sqrt{k_{ref}^{-2}\nabla_{\perp}^2 + n^2(x,y,z)}.$$
(3)

and let

$$n^2(x,y,z) = \gamma_0(x,y,z) + \varepsilon\gamma_1(x,y,z),$$
(4)

where γ_0 is the square of the index of refraction of the background state, and γ_1 is a perturbation scaled by an arbitrary small parameter ε. Following the derivations shown in [8], one can find the next higher-order tangent linear PE solution, which unifies two other less accurate tangent linear solutions proposed by Hursky et al. [9] and Smith [10].

$$u(x + \Delta x, y, z) \cong e^{ik_{ref}\Delta x\mathcal{L}_0}\left[1 + \frac{ik_{ref}}{2}\Delta x(1 - \mathcal{L}_0)\varepsilon\gamma_1\right]u(x,y,z),$$
(5)

where $\mathcal{L}_0 = -1 + \sqrt{k_{\mathrm{ref}}^{-2}\nabla_\perp^2 + \gamma_0(x,y,z)}$ is the background PE operator.

From Eq. (5), we can deduce the sensitivity of sound pressure with respect to n^2 to be

$$\frac{\partial p(\vec{x})}{\partial n^2(\vec{x})} = \frac{ik_{\mathrm{ref}}}{2}\,(2 - \mathcal{L}_0)\,p(\vec{x}) \qquad (6)$$

,

and with the chain rule we can also get $\dfrac{\partial p(\vec{x})}{\partial c(\vec{x})} = -ik_{ref}\,\dfrac{n^2(\vec{x})}{c(\vec{x})}(2-L_0)p(\vec{x})$. This sensitivity kernel is in fact the local kernel at the perturbation location. To obtain the kernel at the receiver location, we can multiply the local kernel with the Green function:

$$\frac{\partial p(\vec{x}_r)}{\partial c(\vec{x})} = G(\vec{x}_r;\vec{x})\frac{\partial p(\vec{x})}{\partial c(\vec{x})} = -ik_{\mathrm{ref}}\,G(\vec{x}_r;\vec{x})\,\frac{n^2(\vec{x})}{c(\vec{x})}\,(2-\mathcal{L}_0)\,p(\vec{x}) \qquad (7)$$

.

WORK COMPLETED

The tasks completed in the year are described below.

1. 3-D sound pressure sensitivity kernel

From the higher-order 3-D tangent linear PE solution, we can deduce a local sound pressure sensitivity kernel shown in Eq. (6). By incorporating the Green's function, we can then extend the local sensitivity kernel to the receiver position. In this year, an adjoint modeling framework has also been implemented to determine the dynamics of the sensitivity kernel associated with the physical oceanographic field. An example showing the sensitivity kernel of sound intensity with respect to sound speed perturbation, $\partial|p|^2/\partial c$, in a nonlinear internal wave field is shown in Figure 1.

2. Joint physical oceanographic and acoustics modeling

A framework has been developed for integrating numerical models of ocean dynamics and acoustics. A data-assimilated ocean model is employed to drive the ocean dynamics in this joint model. An example of sound propagation on a shelfbreak in the Mid-Atlantic Bight is shown in Figure 2. One can see that the original down-slope propagation pattern changes to water-borne ducting due to the change of water column stratification. This examples demonstrates the use of this integrated numerical technical for studying the 3-D sound propagation effects caused jointly by physical oceanographic processes and marine geological variability.

3. Engineering test in the New England Mud Patch area

The PI also joined an engineering test on the New England Mud Patch, south of Martha's Vineyard, MA for examing propagation conditions of broadband acoustic pulses generated by a combustive sound source deployed by ARL:UT. One of the hydrophone arrays deployed in this test was provided by the PI and the acoustics group at WHOI. Preliminary acoustic data and model analyses are shown in Figure 3. Sound propagation models in two different sediment types of environments are shown in Figuers 3(a) and 3(b). The sound source in this modeling study is placed close to the seafloor. In Figure 3(a), the sediment layer is modeled as fine-granted sediment (mud) with compressional wave

speed less than the sound speed in the bottom of water. In Figure 3(b), the sediment layer is modeled as sand with higher compressional wave speed. The model clearly shows that the acoustic energy can be trapped in the lower speed mud layer. A preliminary broadband pulse data and model comparison is shown in Figures 3(c) and 3(d). In Figure 3(c), the spectrograms of received pulses on the hydrophone array are shown, along with time series plots in the bottom panel. In Figure 3(d), results from a broadband sound propagation model are shown. The sediment layer in the model is made to be mud. Despite the very low frequency ground waves, this preliminary model adequately reproduces the pulse dispersion over a broad frequency range.

RESULTS

The major results of this project accomplished in this year are summaried here, along with a publication list provided later. First, A higher-order tangent linear PE solution of 3D sound propagation has been derived, and it unifies other tangent linear PE solutions. This higher-order tangent linear solution also yields a sensitivity kernel of sound pressure variations due to changes in medium sound speed. An adjoint modeling has also implemented to study the dynamics of the sensitivity kernel associated with the physical oceanographic field. A numerical example of 3-D sound pressure sensitivity analysis in a nonlinear internal wave field is presented (Figure 1).

A numerical model has also been constructed to include the sub-bottom layering structure of the New Jersey shelf. The purpose of this model is to investigate the 3-D sound propagation effects caused jointly by marine geological features and oceanographic dynamics in shallow water. Aligning with this research topic, the PI joined an engineering test on the New England Mud Patch for a preliminary sound propagation study. The initial data analysis and modeling effort is presented in Figure 3. In addition to that, ambient noise analysis has been initiated. Figure 4 shows the noise spectrum level during container ships passing by the acoustic engineering test site. The nominal closest-point-of-approach (CPA) distance to the hydrophone array was about 5 to 7 km. The hydrophone deployment was 5.5 days, and the noise spectrum within a 2 hour time window around every CPA are analyzed. Total 35 containers were detected acoustically, and the total analyzed time for the ambient noise was 65 hours long. In Figure 4, the black lines denote the mean and one standard deviation curves. The color curves are the average levels of heavy, moderate and light shipping noise in deep ocean [11]. The analysis suggests that when the big container ships pass by, the ambient noise can reach up to 110 dB re 1μ Pa at frequencies around 100 Hz, which is 30 dB more than the average level in deep ocean reported by Urick [11] for heavy shipping.

IMPACT/APPLICATIONS

The potential relevance of this work to the Navy is on increasing the capability of sonar systems in shallow water areas. The contributions of the effort on studying 3-D sound propagation effects will also be on assessing the environment-induced acoustic impacts.

RELATED PROJECTS

Experimental data used in this project were collected from the ONR SW06 and QPE projects and one of the the reconnaissance cruises on the New England Mud Patch. In addition, strong collaborations have been initiated and continued between the PI's of an ONR MURI project on integrated ocean dynamics and acoustics.

REFERENCES

[1] Y.-T. Lin and J.F. Lynch, "Analytical study of the horizontal ducting of sound by an oceanic front over a slope," *J. Acoust. Soc. Am.*, vol. 131, pp. EL1-EL7 (2012).

[2] Y.-T Lin, T.F. Duda and J.F. Lynch, "Acoustic mode radiation from the termination of a truncated nonlinear internal gravity wave duct in a shallow ocean area," *J. Acoust. Soc. Am.*, vol. 126, pp. 1752-1765 (2009).

[3] Y.-T. Lin, K.G. McMahon, J.F. Lynch, and W.L. Siegmann, "Horizontal ducting of sound by curved nonlinear internal gravity waves in the continental shelf areas," *J. Acoust. Soc. Am.*, vol. 133, pp. 37-49 (2013).

[4] Y.-T. Lin, T.F. Duda, and A.E. Newhall, "Three-dimensional sound propagation models using the parabolic-equation approximation and the split-step Fourier method," *J. Comp. Acoust.*, vol. 21, 1250018 (2013).

[5] Y.-T. Lin and T.F. Duda, "A higher-order split-step Fourier parabolic-equation sound propagation solution scheme," *J. Acoust. Soc. Am*, vol. 132, pp. EL61-EL67 (2012).

[6] Y.-T. Lin, J.M. Collis and T.F. Duda, "A three-dimensional parabolic equation model of sound propagation using higher-order operator splitting and Padé approximants," *J. Acoust. Soc. Am.*, vol. 132, pp. EL364-370 (2012).

[7] F. D. Tappert, "Parabolic equation method in underwater acoustics", *J. Acoust. Soc. Am.*, vol. 55, p. S34 (1974).

[8] Y.-T. Lin, "A higher-order tangent linear parabolic-equation solution of three-dimensional sound propagation," *J. Acoust. Soc. Am.*, vol. 134, pp. EL251-EL257 (2013).

[9] P. Hursk, M. B. Porter, B. D. Cornuelle, W. S. Hodgkiss, and W. A. Kuperman, "Adjoint modeling for acoustic inversion," *J. Acoust. Soc. Am.*, vol. 115, 607–619 (2004)

[10] K. B. Smith, "Adjoint modeling with a split-step Fourier parabolic equation model (L)," *J. Acoust. Soc. Am.*, vol. 120, 1190–1191 (2006).

[11] Urick, Robert, Principles of Underwater Sound, International Edition (McGraw-Hill, Inc.), Chap. 7, 1993.

PUBLICATIONS

2015 B.J. DeCourcy, **Y.-T. Lin**, and W.L. Siegmann, "Approximate formulas and physical interpretations for horizontal acoustic modes in a shelf-slope front model," *J. Acoust. Soc. Am. Express Letter*, [submitted, referred]

2015 A.A. Shmelev, J.F. Lynch and **Y.-T. Lin**, "Low frequency acoustic propagation through crossing internal waves in shallow water," *J. Acoust. Soc. Am.*, [submitted, referred]

2015 **Y.-T. Lin**, "3-D Shallow Water Acoustics," in Seabed and Sediment Acoustics: Measurements and Modelling 2015, Institute of Acoustics, University of Bath, UK, Sept. 7-9 2015. [published, not refereed]

2015 **Y.-T. Lin**, T.F. Duda, C. Emerson, G.G. Gawarkiewicz, A.E. Newhall, B. Calder, J.F. Lynch, P. Abbot, Y.-J. Yang and S. Jan, "Experimental and numerical studies of sound propagation over a

submarine canyon northeast of Taiwan," *IEEE J. Ocean. Eng.*, vol. 40, pp. 237-249. [published, refereed]

2014 C. Emerson, J.F. Lynch, P. Abbot, **Y.-T. Lin**, T.F. Duda, G.G. Gawarkiewicz and C.-F. Chen, "Acoustic Propagation Uncertainty and Probabilistic Prediction of Sonar System Performance in the Southern East China Sea Continental Shelf and Shelfbreak Environments," *IEEE J. Ocean. Eng.*, Early Access (2014). DOI: 10.1109/JOE.2014.2362820 [published, refereed]

2014 **Y.-T. Lin**, " Numerical applications of a higher order square-root Helmholtz operator splitting method on modeling three-dimensional sound propagation," in Proceedings of the 2nd International Conference and Exhibition on Underwater Acoustics, June 22-27, 2014, Rhodes, Greece. [published, not refereed]

2014 A.A. Shmelev, J.F. Lynch, **Y.-T. Lin** and H. Schmidt, "3D coupled mode analysis of internal-wave acoustic ducts," *J. Acoust. Soc. Am.*, vol. 135, pp. 2497-2512. [published, refereed]

2014 L.Y.S. Chiu, A. Chang, **Y.-T. Lin**, and C.-S. Liu, "Estimating Geo-acoustic Properties of the Surficial Sediments in the Region of North Mein-Hua Canyon with a Chirp Sonar Profiler," *IEEE J. Ocean. Eng.*, Early Access. DOI:10.1109/JOE.2013.2296362 [published, refereed]

2014 **Y.-T. Lin**, "Numerical modeling of three-dimensional underwater sound propagation under rough sea surfaces," *J. Acoust. Soc. Am.*, vol. 135, p. 2429. [published, not refereed]

2013 **Y.-T. Lin**, W. G. Zhang, and T. F. Duda, "Sensitivity of the underwater sound field in submarine canyons to water column variability," *J. Acoust. Soc. Am.*, vol. 134, p. 4114. [published, not refereed]

2013 **Y.-T. Lin**, "A higher-order tangent linear parabolic-equation solution of three-dimensional sound propagation," *J. Acoust. Soc. Am.*, vol. 134, pp. EL251-EL257. [published, refereed]

2013 **Y.-T. Lin**, K.G. McMahon, J.F. Lynch, and W.L. Siegmann, "Horizontal ducting of sound by curved nonlinear internal gravity waves in the continental shelf areas," *J. Acoust. Soc. Am.*, vol. 133, pp. 37-49. [published, refereed]

2013 M.E.G.D. Colin, T.F. Duda, L.A. te Raa, T. van Zon, P.J. Haley Jr., P.F.J. Lermusiaux, W.G. Leslie, C. Mirabito, F.P.A. Lam, A.E. Newhall, **Y.-T. Lin**, and J.F. Lynch, "Time-evolving acoustic propagation modeling in a complex ocean environment," in Proceedings of Oceans '13 (Bergen) Conference, IEEE/MTS. [published, not refereed]

2013 T.F. Duda, **Y.-T. Lin** and B. D. Cornuelle, Scales of time and space variability of sound fields reflected obliquely from underwater slopes, Proc. Meet. Acoust., 19, 070025. [published, not refereed]

2013 J.F. Lynch, **Y.-T. Lin**, T. F. Duda and A. E. Newhall, "Characteristics of acoustic propagation and scattering in marine canyons", in Proceedings of the 1st International Underwater Acoustics Conference, Corfu, Greece. [published, not refereed]

HONORS/AWARDS/PRIZES

Recipient: Ying-Tsong Lin
Recipient's Institution: Woods Hole Oceanographic Institution
Award Name A. B. Wood Medal and Prize of the Institute of Acoustics
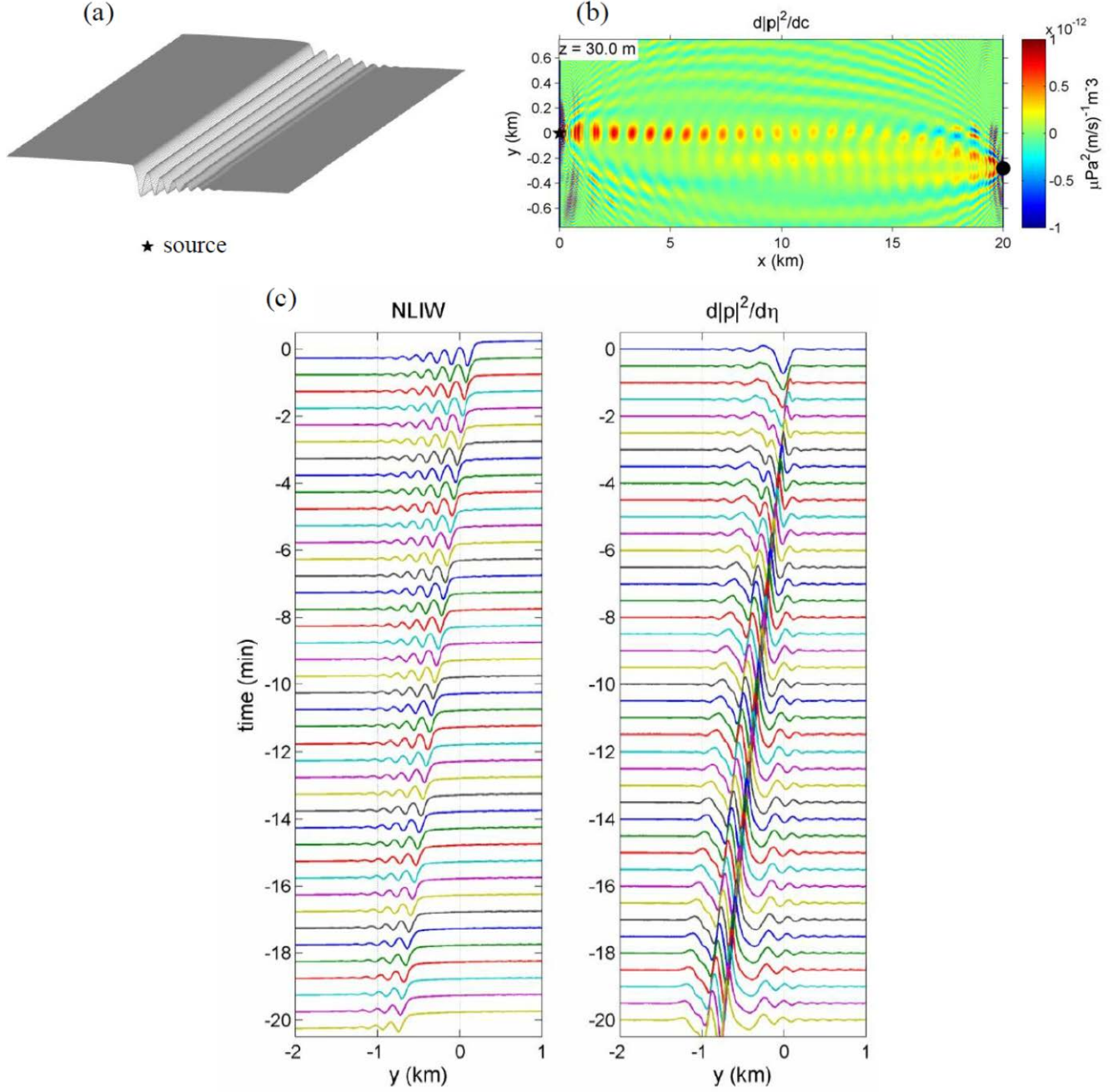Award Sponsor: Institute of Acoustics

Figure 1: Sensitivity analysis of an internal wave acoustic duct.
[(a) internal wave displacement (the source is underneath the first wave crest), (b) the sensitivity kernel of sound pressure square with respect to sound speed perturbation between the source and a receiver underneath the second wave crest, and (c) the sound pressure sensitivity and its dynamics following the internal wave motion. The sensitivity kernel has been converted to be per wave height through a chain rule.]
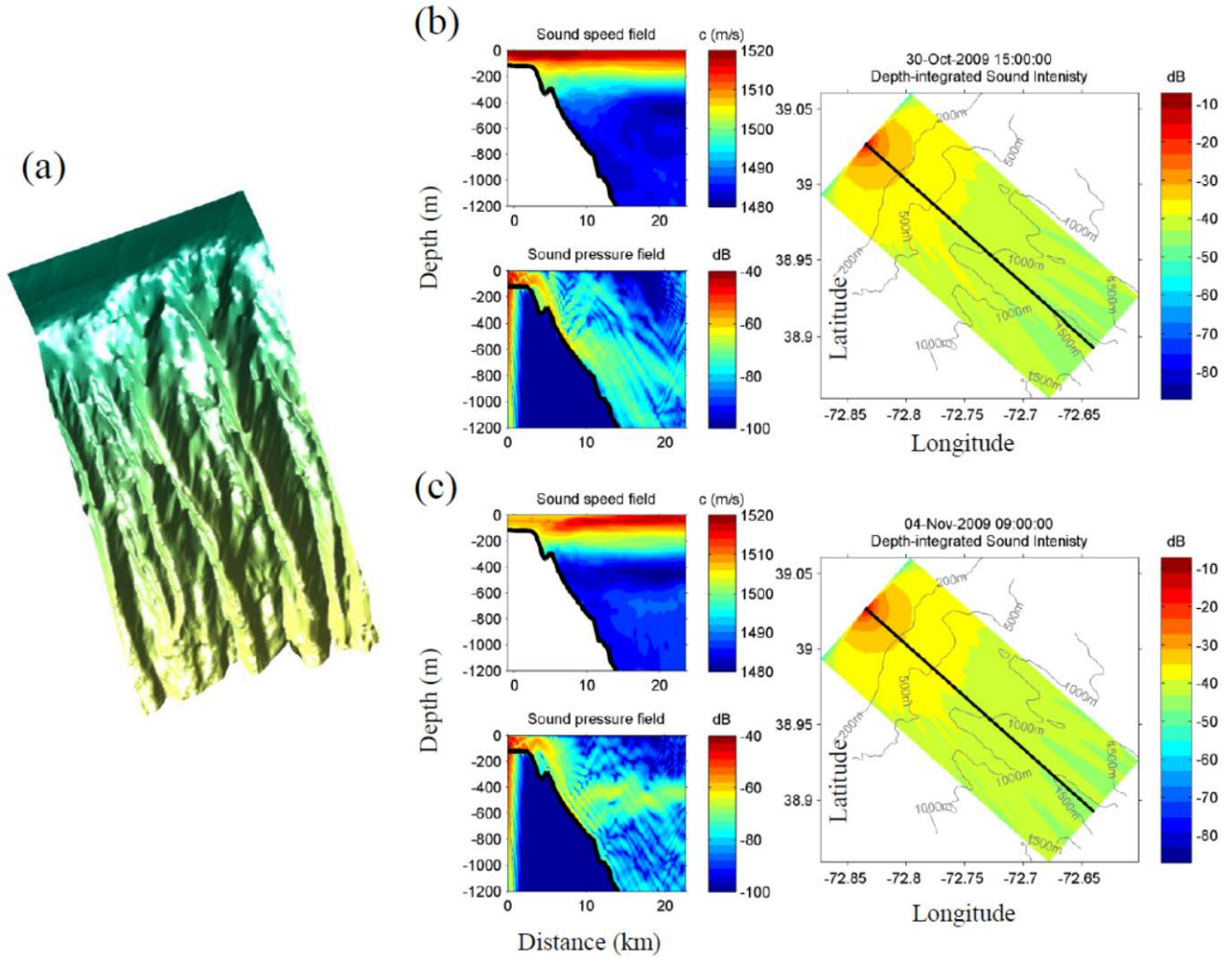
Figure 2: Integrated numerical simulations of ocean dynamics and acoustics on the slope of the New Jersey Shelf.
[(a)The bathymetry, (b) the original down-slope propagation pattern, and (c) change of propagation pattern to water-borne ducting due to water column variability. The beam pattern on the depth integrated sound intensity plots on the right shows the 3-D focusing of sound by the small canyons on the slope.]
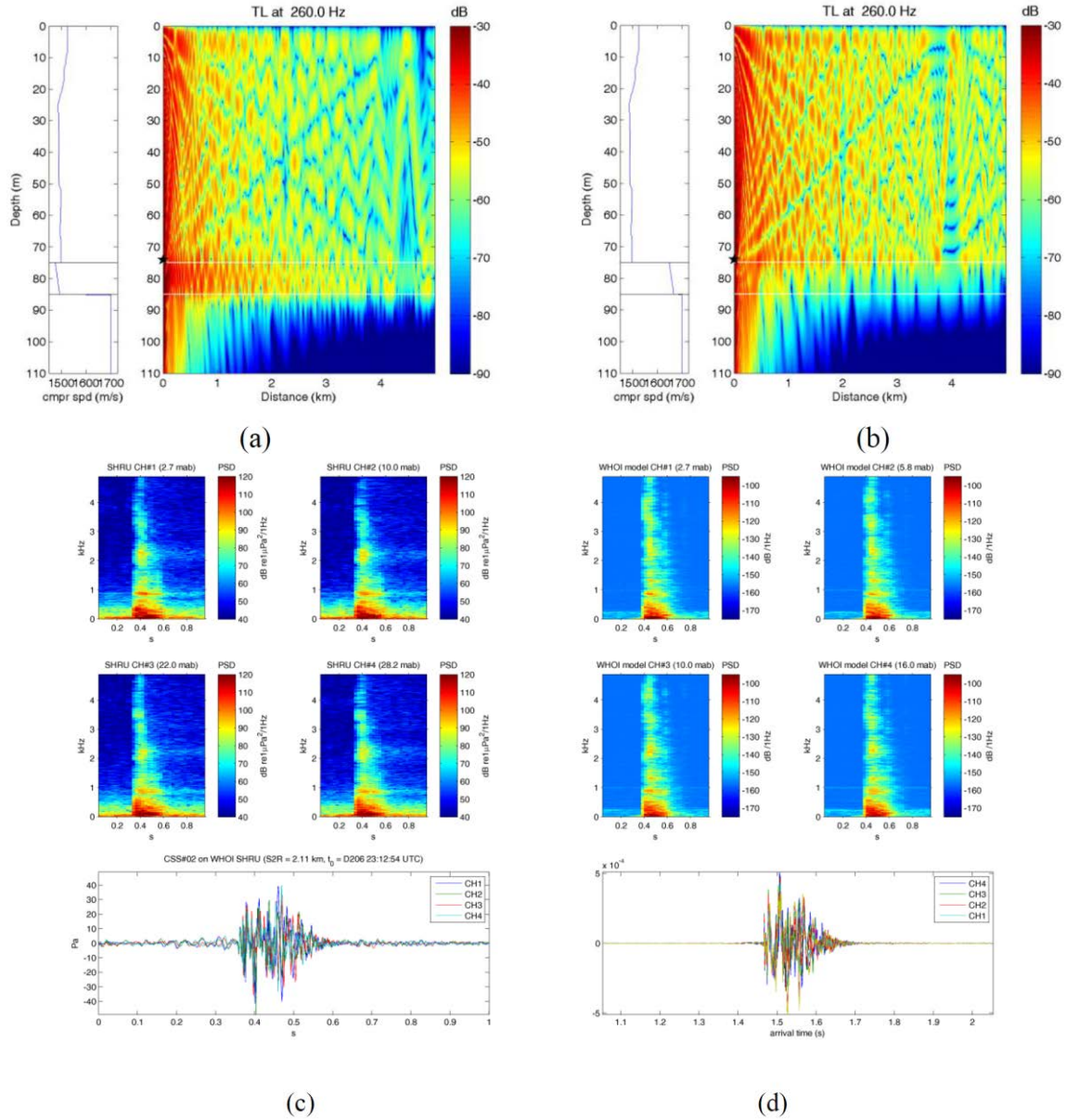
Figure 3: Preliminary acoustic data and model analyses in the engineering test conducted on the New England Mud Patch.

[(a) and (b) Sound propagation models in two different sediment types of environments. The sound source in this model study is placed close to the seafloor. In the panel (a), the sediment layer is modeled as fine-granted sediment (mud) with compressional wave speed less than the sound speed in the bottom of water column. In the panel (b), the sediment layer is modeled as sand with higher compressional wave speed. One can see that the acoustic energy can be trapped in the lower speed mud layer. (c) and (b) Preliminary broadband pulse data and model comparison. In the panel (c), the spectrograms of received pulses on four hydrophones close to the bottom are shown, along with time series plots in the bottom panel. The broadband source was made available by D. Knobles of ARL:UT, and the hydrophone array data was provided by the ocean acoustics group at WHOI. In the panel (d), results from a broadband sound propagation model are shown. The sediment layer in the model is made to be mud. Despite the very low frequency ground waves, this preliminary model adequately reproduces the pulse dispersion over a broad frequency range.]
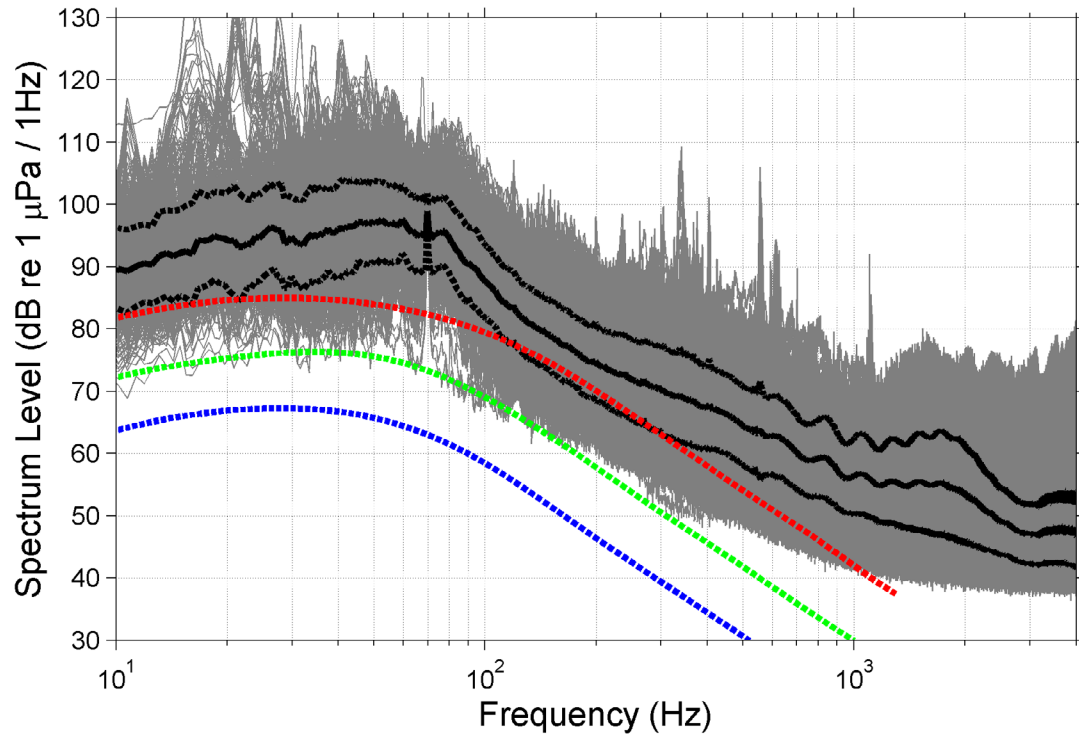
Figure 4. Ambient noise spectrum level during container ships passing by the acoustic engineering test site on the New England Mud Patch.
[The hydrophone deployment was 5.5 days, and the noise spectrum level curves within a 2 hour time window around every closest approach point of the container to the hydrophone array are shown. Total 35 containers were detected acoustically, and the total analyzed time for the ambient noise was 65 hours long. The black lines denote the mean and one standard deviation curves. The color curves are the average levels of heavy, moderate and light shipping noise in deep ocean (11).]